

# An Analysis of High-Power Transmission from DSN Antennas and Aircraft Certification Limits

Vahraz Jamnejad\*

**ABSTRACT.** — This work addresses the issue of calculating the power density ( $\text{W}/\text{m}^2$ ) and field intensity ( $\text{V}/\text{m}$ ) distribution of NASA's Deep Space Network (DSN) large reflector antennas in the Fresnel (near- to middle-field zone) as a function of the distance from the antenna and the off-axis angles. The calculation uses a simplified scalar method for radiation from circular apertures. The emphasis in this article is on the impact of the near- to mid-zone fields of DSN antennas on compliance with aircraft certification limits. The region of particular interest is the approximate range of 200 m to 30 km, which falls in the mid-field or Fresnel zone of the 34-m and 70-m antennas of the DSN.

## I. Introduction

The high-intensity radio frequency (HIRF) obtained from the high-power transmissions from large Deep Space Network (DSN) antennas with 34-m-diameter and 70-m-diameter apertures should be considered in compliance with aircraft certification limits.

The DSN radiation environment is rather unique. It is characterized by large antennas (34 m and 70 m in diameter) mechanically steered and slow moving, with transmitters of up to 500 kW of power and very narrow beams (so-called pencil beams).

Figure 1 shows a simple model of radiation from a large reflector antenna such as a DSN antenna. The highest field intensity is obtained along the main axis (boresight) of the antenna; the field initially oscillates rapidly with a constant field intensity envelope twice that of the average value on the aperture (and a power density four times or 6 dB above the aperture average). The last peak of the field intensity along the main axis is achieved at a distance of  $d_c = D^2/4\lambda$  (which we call the characteristic distance), and from that point on the field decreases rather uniformly towards the far field. However, the average field intensity across the antenna beam is lower than the peak values along the main axis, as will be seen.

---

\* Communications Ground Systems Section.

The research described in this publication was carried out by the Jet Propulsion Laboratory, California Institute of Technology, under a contract with the National Aeronautics and Space Administration. © 2014 California Institute of Technology. U.S. Government sponsorship acknowledged.

As a beam of electromagnetic energy, the field approximately stays like a cylindrical beam to about  $2(D^2/4\lambda) = 2d_c$  and then gradually approaches the cone of the far-field beam with a null-to-null beamwidth of approximately  $\theta \cong 1/(D/\lambda) = D/(D^2/\lambda)$  radians.

There are, in general, three zones: a very near-field, near- to mid-field (Fresnel zone), and the far-field zone (Figure 1). The near and part of the mid field are modeled as a cylinder with a diameter equal to antenna aperture diameter. The far-field zone is modeled as a cone centered at the antenna and a transition zone between the near-field and far-field zones.

The detailed structure of the field is quite complex and varies as a function of the antenna diameter and transmitter frequency, as shown in the Appendix, and as also shown in the figures later in this section.

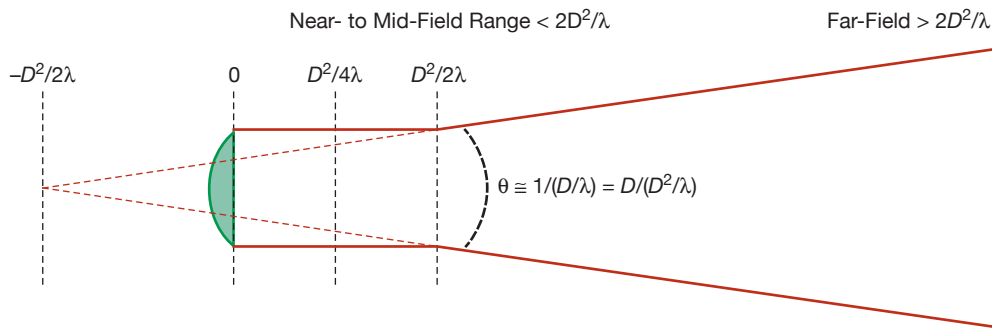


**Figure 1. Model of radiation from a DSN antenna.**

The detailed and very accurate calculation of the fields of these large antennas using rigorous electromagnetic (EM) analysis techniques is very time consuming and is the subject of other studies. However, as explained in the Appendix, we have made a number of simplifying assumptions in obtaining the presented fields, which we believe is sufficient for the purposes of this article.

We will present color contours of the fields in regions of interest for several cases of interest. We will also provide linear plots of the field along the main axis of the antenna as well as an average field calculated on the cross section of the antenna beam, again for several cases of interest. But before presenting the field results, a discussion of the averaging concept and technique is in order.

## II. Field Averaging

Although the peak value of the field might be of interest in some special cases (e.g., a hovering helicopter), for most cases of interest an aircraft or rotorcraft is moving with a certain speed through the antenna beam, and the average field over a given period of time and the corresponding travelled distance may be of greater significance. The worst-case scenario involves crossing the beam through its center. The angle of the direction of travel with the direction of the beam axis must also be taken into account for the distance travelled.

Table 1 shows the beam-crossing times for the near-field beam of a 34-m antenna for a variety of antenna elevation angles (10 to 90 deg) and plane speed of 100 to 350 knots or rotorcraft speed of 50 to 150 knots. (Each knot is 1 nautical mile/hr or 1.852 km/hr or 0.51444 m/s). It assumes:

- The craft flies horizontally. (Planes usually do. Even when they ascend/descend, they are restricted to a 3-deg slope except for emergencies.)
- The DSN obeys the regulatory limit of no high-power radiation at elevation angles of less than 10 deg. (The DSN has in-place multiple lock mechanisms to assume that.)
- The crossing is through the center of the beam, the longest crossing time, and hitting the peak of the beam.

Table 1 shows that for a 34-m antenna, for the majority of cases (highlighted in green), the crossing time is under 1 s. Under the worst-case scenario (10-deg antenna elevation and a slow plane at 100 knots), the crossing time can extend to 4 s. The reason 1-s averaging is highlighted is that it is the averaging time used by the Federal Aviation Administration (FAA).

**Table 1. Maximum beam-crossing times in seconds for the 34-m near-field beam.**

Antenna Elevation, deg	Speed, knots						
	50	100	150	200	250	300	350
10	7.612	3.806	2.537	1.903	1.522	1.269	1.087
20	3.865	1.932	1.288	0.966	0.773	0.644	0.552
30	2.644	1.322	0.881	0.661	0.529	0.441	0.378
40	2.056	1.028	0.685	0.514	0.411	0.343	0.294
50	1.726	0.863	0.575	0.431	0.345	0.288	0.247
60	1.526	0.763	0.509	0.382	0.305	0.254	0.218
70	1.407	0.703	0.469	0.352	0.281	0.234	0.201
80	1.342	0.671	0.447	0.336	0.268	0.224	0.192
90	1.322	0.661	0.441	0.330	0.264	0.220	0.189

For a 70-m antenna, the near-field cylinder has a diameter approximately twice as long, so the crossing times are approximately twice as long and are given in Table 2.

To begin with, we compute the average field normal to the main axis and across the center of the beam to a width of  $D$  (diameter of the antenna) for any given distance from the aperture. Due to relatively slow field variation along the beam (in units of beam diameter  $D$ ), this averaging is reasonable even for non-normal angles of crossing the beam.

Using the 1-s criterion as the acceptable averaging time, the average field value defined above (across the beam of width  $D$ ), provides a conservative and acceptable value. However, for slower craft and/or lower elevation angles, the 1-s criterion might require averaging over a shorter distance across the center of the beam. The crossing distances based on the 1-s criteria are shown in Table 3. In this case, the averaging distances required for a 34-m antenna are shown in light green background, while those for 70-m antenna are shown in

light and dark shades of green. Averaging based on the crossing distance for a given time criteria will require additional calculations, which will be done in a future article.

**Table 2. Maximum beam-crossing times in seconds for the 70-m near-field beam.**

Antenna Elevation, deg	Speed, knots						
	50	100	150	200	250	300	350
10	15.672	7.836	5.224	3.918	3.134	2.612	2.239
20	7.957	3.978	2.652	1.989	1.591	1.326	1.137
30	5.443	2.721	1.814	1.361	1.089	0.907	0.778
40	4.234	2.117	1.411	1.058	0.847	0.706	0.605
50	3.553	1.776	1.184	0.888	0.711	0.592	0.508
60	3.142	1.571	1.047	0.786	0.628	0.524	0.449
70	2.896	1.448	0.965	0.724	0.579	0.483	0.414
80	2.763	1.382	0.921	0.691	0.553	0.461	0.395
90	2.721	1.361	0.907	0.680	0.544	0.454	0.389

**Table 3. Distance in meters crossed through the near-field beam in 1 s.**

Antenna Elevation, deg	Speed, knots						
	50	100	150	200	250	300	350
10	4.467	8.933	13.400	17.866	22.333	26.800	31.266
20	8.798	17.595	26.393	35.190	43.988	52.785	61.583
30	12.861	25.722	38.583	51.444	64.306	77.167	90.028
40	16.534	33.068	49.602	66.136	82.670	99.204	115.737
50	19.704	39.409	59.113	78.817	98.522	118.226	137.931
60	22.276	44.552	66.828	89.104	111.380	133.657	155.933
70	24.171	48.342	72.513	96.684	120.855	145.026	169.197
80	25.331	50.663	75.994	101.326	126.657	151.989	177.320
90	25.722	51.444	77.167	102.889	128.611	154.333	180.056

### III. Field Intensity Evaluation

Now we calculate and plot the distributed field, peak field, and average field as defined above for typical DSN transmitters.

As mentioned previously, using a relatively simple scalar approximation for the calculation of the fields from an aperture antenna with circular symmetry (see the Appendix), we provide the fields for five different cases:

- (1) 34-m antenna at 7.1675 GHz (X-band) with 80 kW transmit power
- (2) 34-m antenna at 2.1 GHz (S-band) with 20 kW transmit power
- (3) 70-m antenna at 2.1 GHz (S-band) with 400 kW transmit power
- (4) 70-m antenna at 7.1675 GHz (X-band) , with 20 kW transmit power
- (5) 70-m antenna at 8.5 GHz (X-band) with 500 kW transmit power

As a reference, the characteristic and far-field distances for these cases are given in Table 4.

**Table 4. Characteristic distance  $d_c = D^2/4\lambda$  and far-field distance  $d_f = 2D^2/\lambda$  for considered cases.**

	34-m, 7.1675 GHz	34-m, 2.1 GHz	70-m, 2.1 GHz	70-m, 7.1675 GHz	70-m, 8.5 GHz
$d_c$	6,910 m	2,025 m	8,581 m	29,288 m	34,733 m
$d_f$	55,276 m	16,196 m	68,648 m	234,301 m	277,859 m

Figures 2(a), 3(a), 4(a), 5(a), and 6(a) show the finer structure of the field, normalized to the field on the aperture surface of the antenna, in dB. The axes are the distance from the center axis of the cylinder, and the distance from the antenna along this axis. Note first that as the distance from the axis reaches the radius of the cylinder, the field drops sharply. Notice further how the field changes from point to point, along the beam well beyond the near field.

Figures 2(b), 3(b), 4(b), 5(b), and 6(b) show the field normalized to reference average voltage limits as specified by the FAA (see Tables 5(a) and 5(b), which also include the calculated results from the following plots).

Figures 2(c), 3(c), 4(c), 5(c), and 6(c) show the peak/maximum field (blue line) along the central axis of the beam and average field (red line), as a function of the distance from the antenna. The peak/maximum oscillates with a maximum envelope twice the average value on the aperture, as shown. The red line shows the average field encountered by a craft crossing the beam perpendicularly. The average is performed over a strip of the width of the antenna.

Figures 2(d), 3(d), 4(d), 5(d), and 6(d) show the average field intensity experienced by a fixed-wing craft over 1 s at 100 knots, crossing the beam at several different beam angles. Notice that in these plots, the envelope of maximum field along the main axis is given.

Finally, Figures 2(e), 3(e), 4(e), 5(e), and 6(e) present the average field intensity experienced by a rotorcraft over 3 s at 50 knots, crossing the beam at several different beam angles. Again, in these plots, the envelope of maximum field along the main axis is given.

These plots can be used in evaluating compliance of the DSN antennas with radiation certification requirements for aircraft.

In the figures, we refer to various Environments I, II, and II. The FAA established radio frequency (RF) field strengths for certification of aircraft and their parts in a HIRF environment. The criteria define the radiation environment the aircraft electrical and electronic systems have to withstand as HIRF Environment I (Certification HIRF Environment), HIRF Environment II (Normal HIRF Environment), and HIRF Environment III (Rotorcraft Severe Environment). See Tables 5(a) and 5(b).

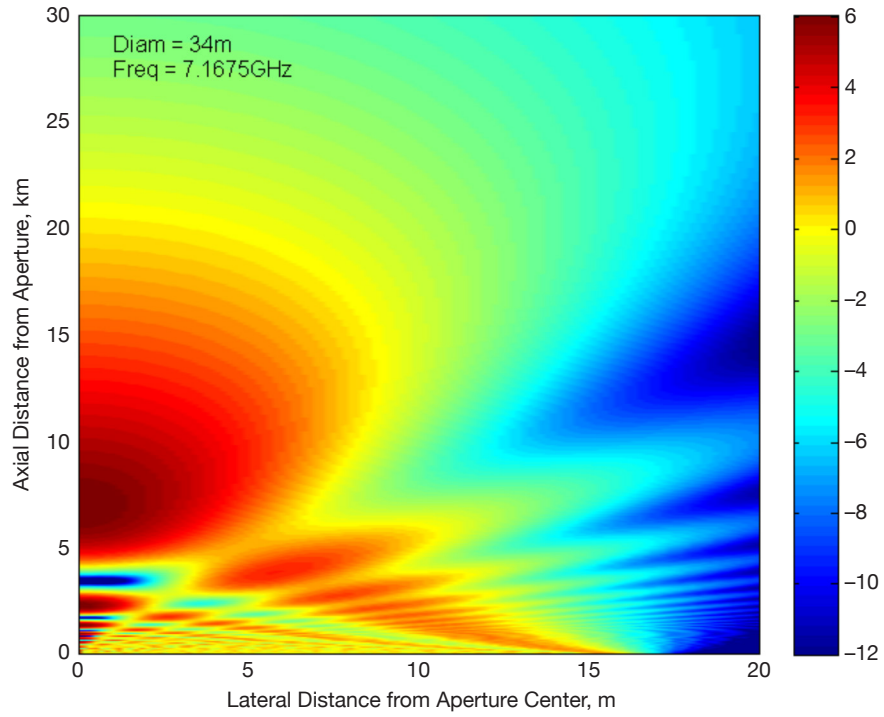


**Figure 2(a). Actual field for X-band transmitter on 34-m antenna: a color plot of normalized field power density in dB for a 34-m circular-aperture antenna at 7.1675 GHz.**

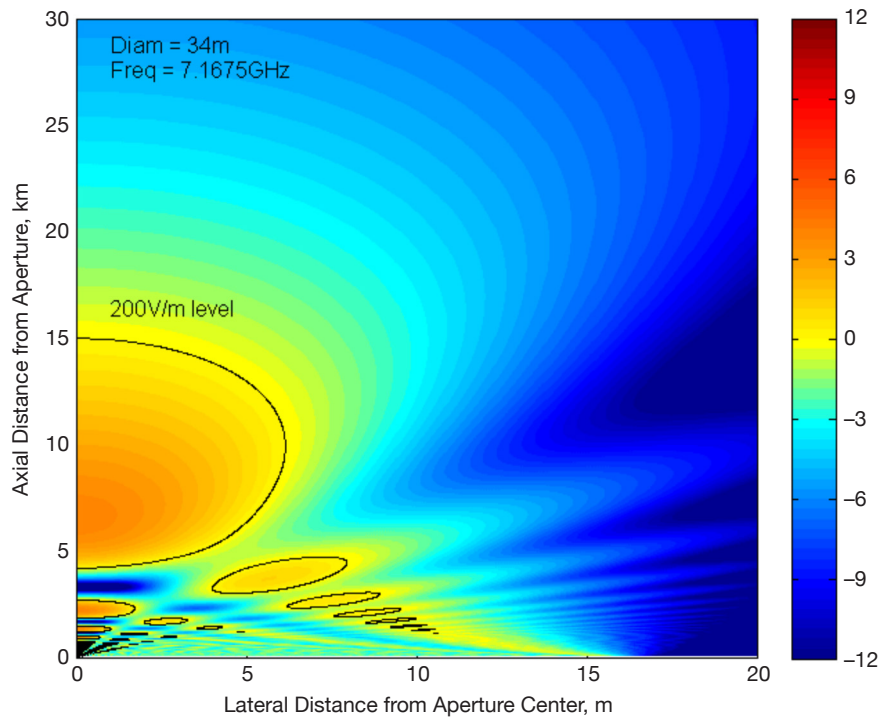


**Figure 2(b). Field structure for 80 kW, X-band, 34-m, referenced to Environment I and III of FAA. Field normalized to 200 V/m in dB for a 34-m circular-aperture antenna with 56800 W power at 7.1675 GHz.**

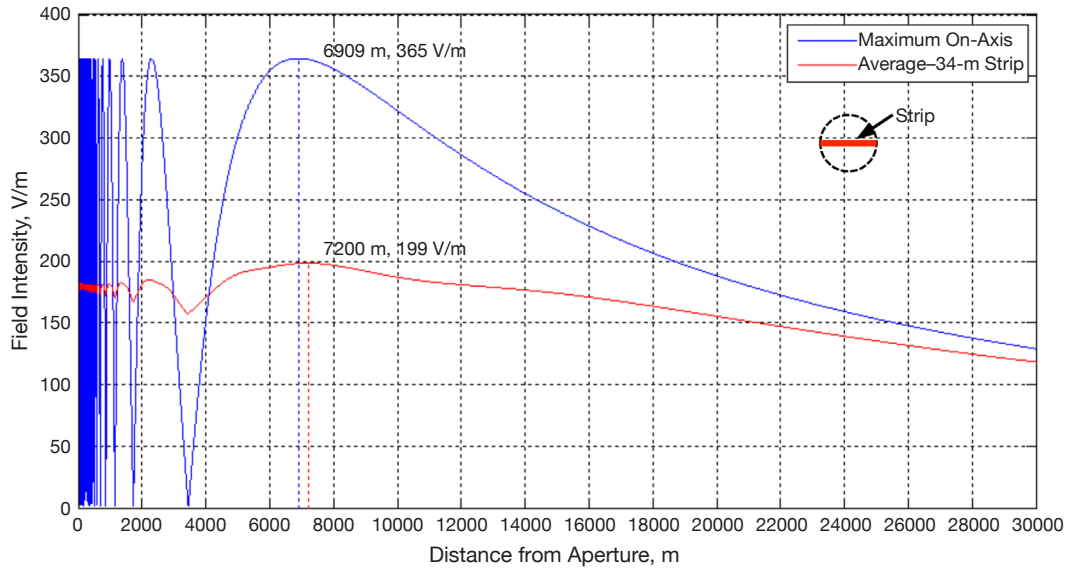


**Figure 2(c). Peak and average field, X-band, 34-m, 80 kW. Averaged field intensity on a cross-section strip of given width for a 34-m-aperture antenna with 80000 W input power at 7.175 GHz.**

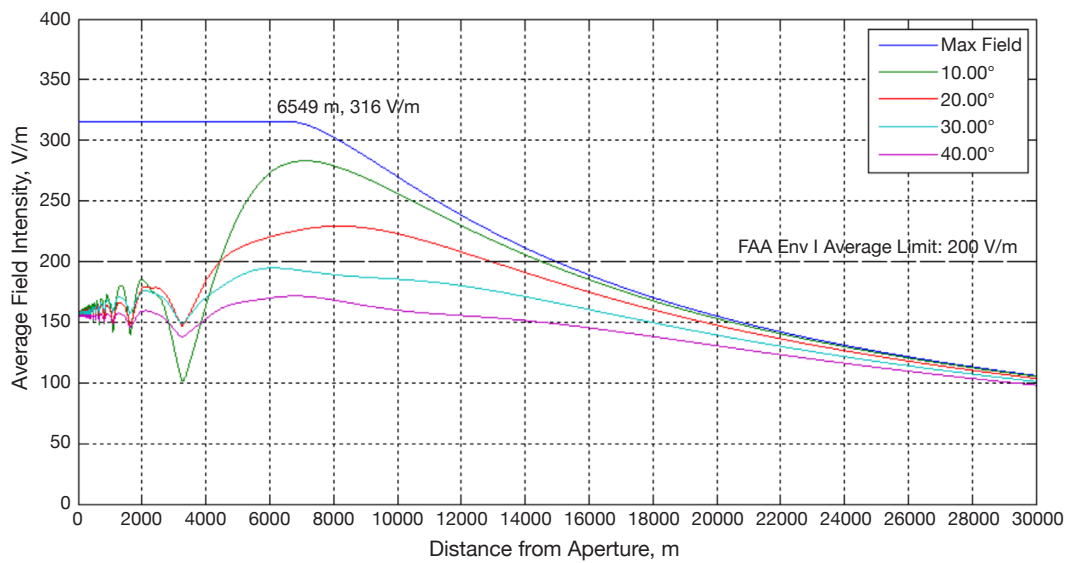


**Figure 2(d). Peak and average field, 80 kW, X-band, 34-m, referenced to Environment I. Averaged field intensity over 1 s experienced by an aircraft at 100 knots, crossing the beam of a 34-m-aperture antenna at given angles (56800 W input power at 7.1675 GHz).**

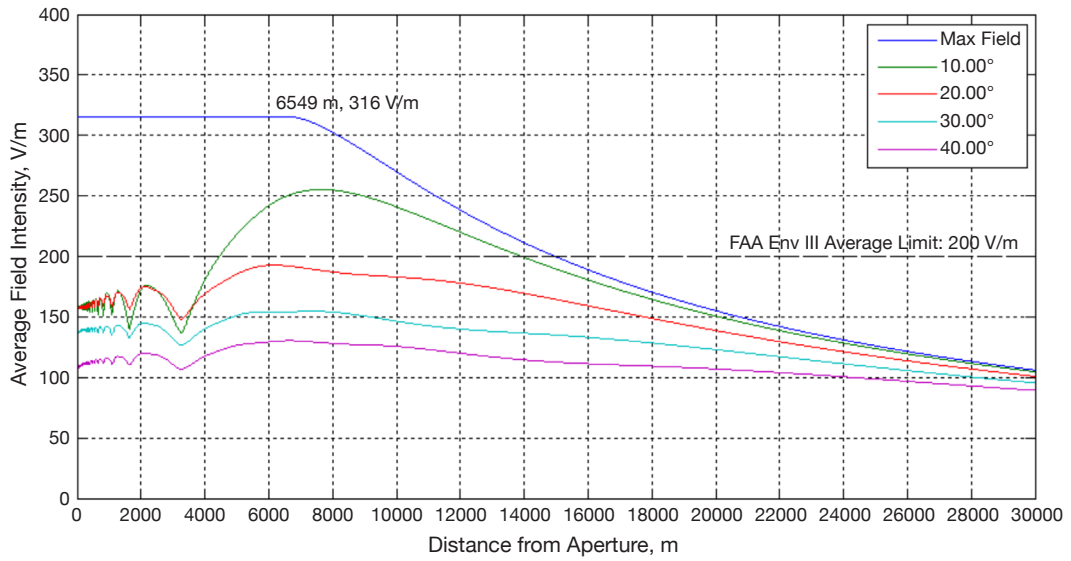


**Figure 2(e). Peak and average field, 80 kW, X-band, 34-m, referenced to Environment III. Averaged field intensity over 3 s experienced by a rotorcraft at 50 knots, crossing the beam of a 34-m-aperture antenna at given angles (56800 W input power at 7.1675 GHz).**

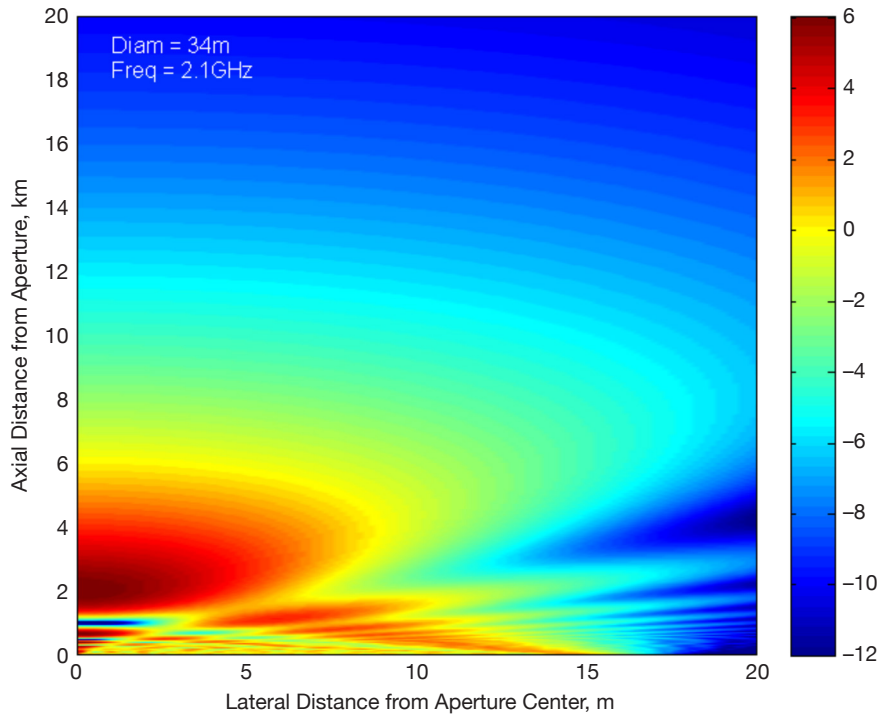


**Figure 3(a). Field structure for 34-m, S-band, 20 kW: a color plot of normalized field power density in dB for a 34-m circular-aperture antenna at 2.1 GHz.**

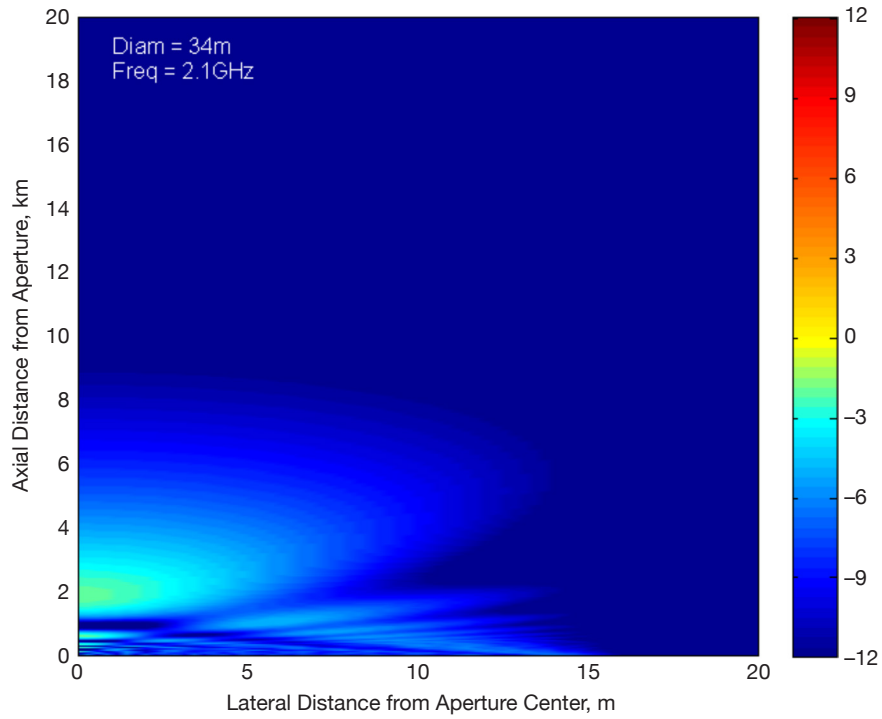


**Figure 3(b).** Field structure for 20 kW, S-band, 34-m, referenced to Environment I. Field normalized to 200 V/m in dB for a 34-m circular-aperture antenna with 14200 W power at 2.1 GHz. The figure for Environment III (490 V/m limit) has even lower relative field values and is not shown.

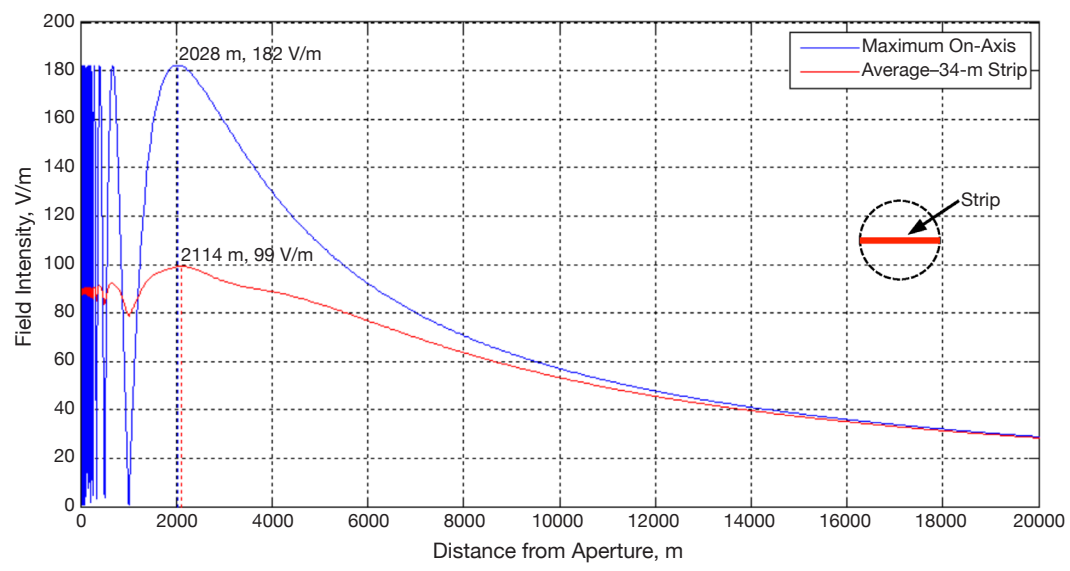


**Figure 3(c).** Maximum and average field for 34-m, S-band, 20 kW. Averaged field intensity on a cross-section strip of given width for a 34-m-aperture antenna with 20000 W input power at 2.1 GHz.

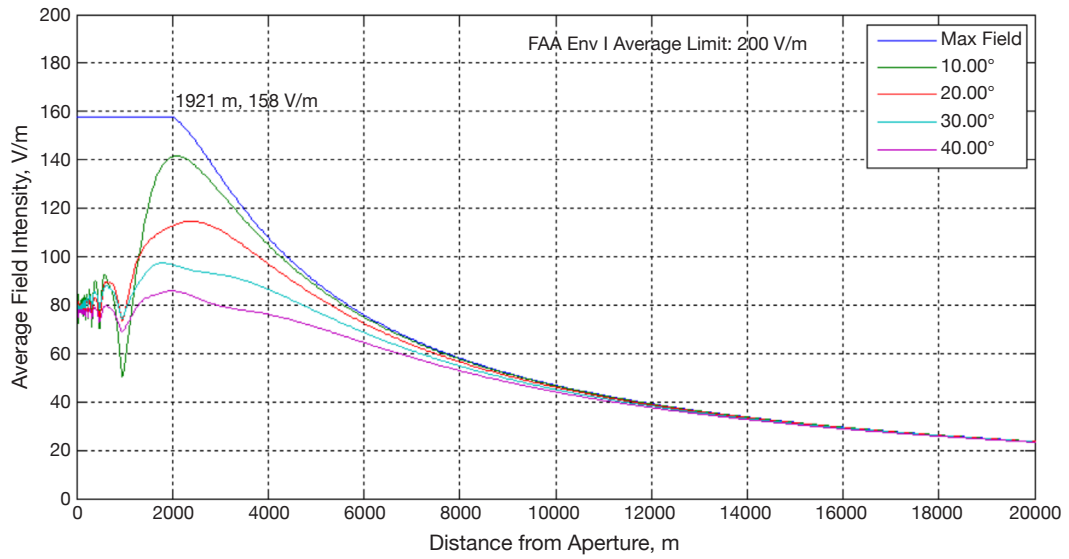


**Figure 3(d). Maximum and average field for 20 kW, S-band, 34-m, referenced to Environment I. Averaged field density over 1 s experienced by an aircraft at 100 knots, crossing the beam of a 34-m-aperture antenna at given angles (14200 W input power at 2.1 GHz).**

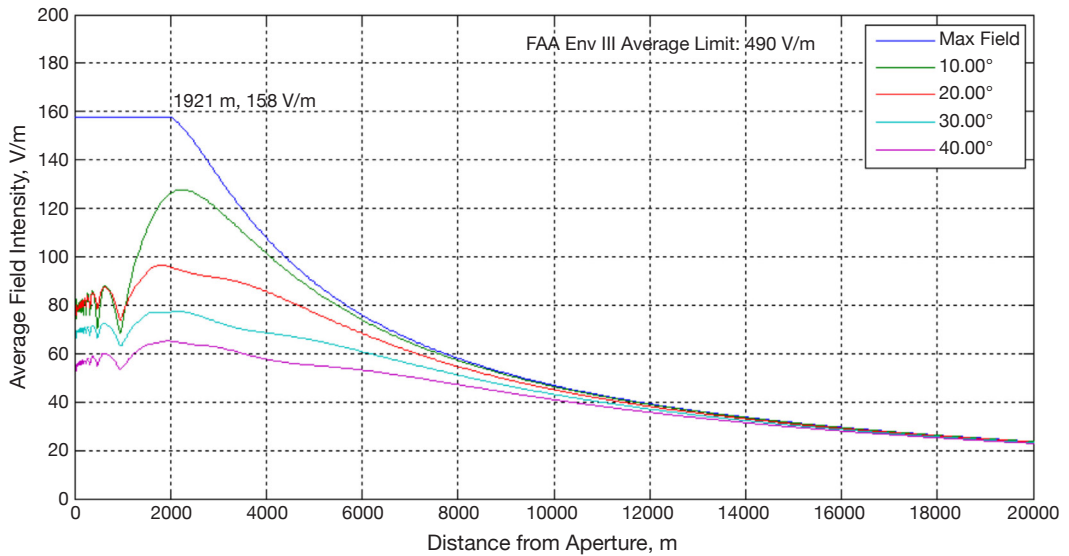


**Figure 3(e). Peak and average field for 20 kW, S-band, 34-m, referenced to Environment III. Averaged field intensity over 3 s experienced by a rotorcraft at 50 knots, crossing the beam of a 34-m-aperture antenna at given angles (14200 W input power at 2.1 GHz).**

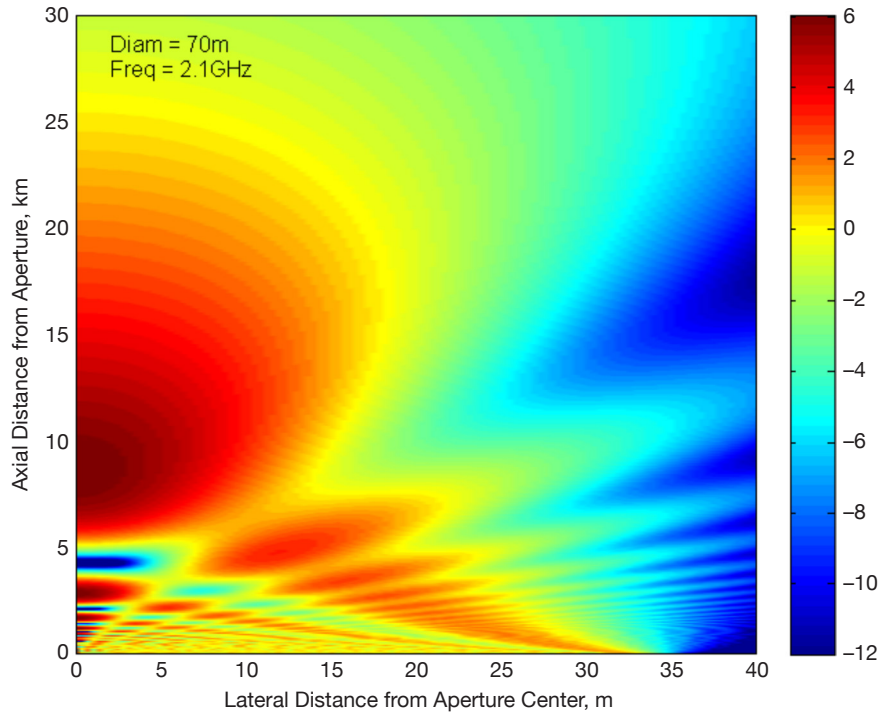


**Figure 4(a).** Field structure for 70-m, S-band, 400 kW: a color plot of normalized field power density in dB for a 70-m circular-aperture antenna at 2.1 GHz.

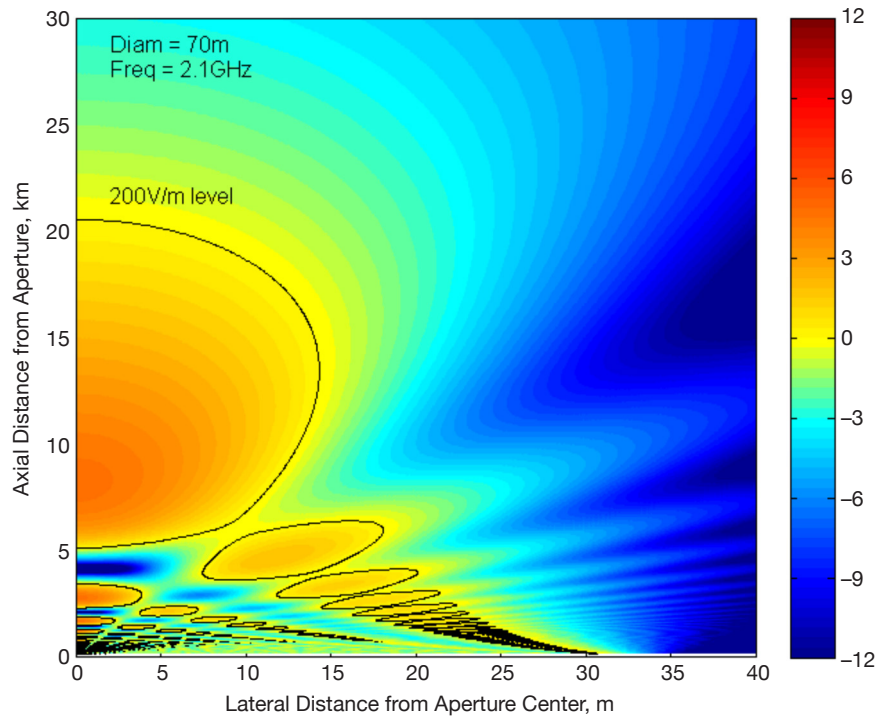


**Figure 4(b).** Field structure for 70-m, S-band, 400 kW, referenced to Environment I. Field normalized to 200 V/m in dB for a 70-m circular-aperture antenna with 284000 W power at 2.1 GHz. The figure for Environment III (490 V/m limit) has even lower relative field values and is not shown.

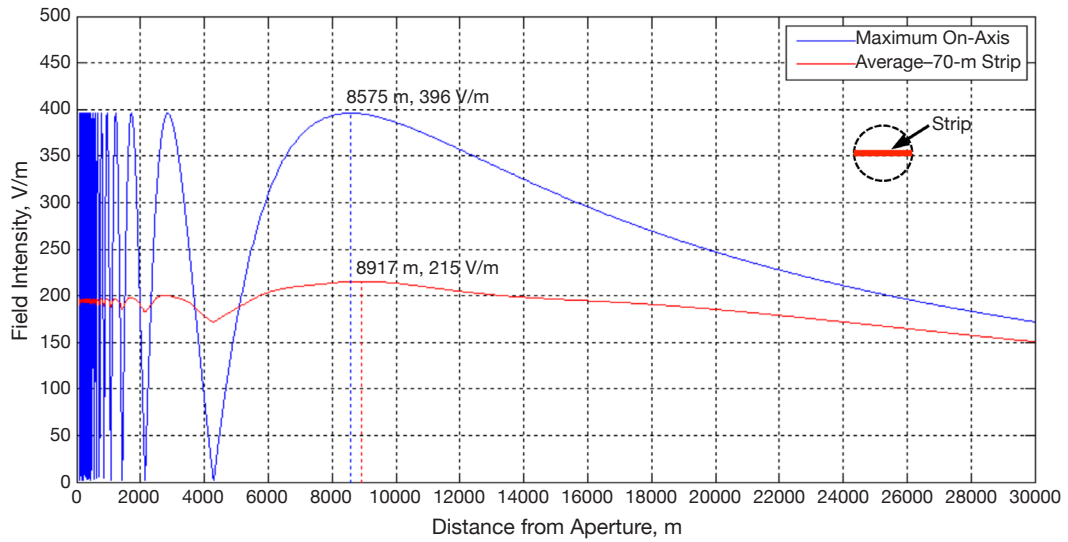


**Figure 4(c). Maximum and average field for 70-m, S-band, 400 kW. Averaged field intensity on a cross-section strip of given width for a 70-m-aperture antenna with 400000 W input power at 2.1 GHz.**

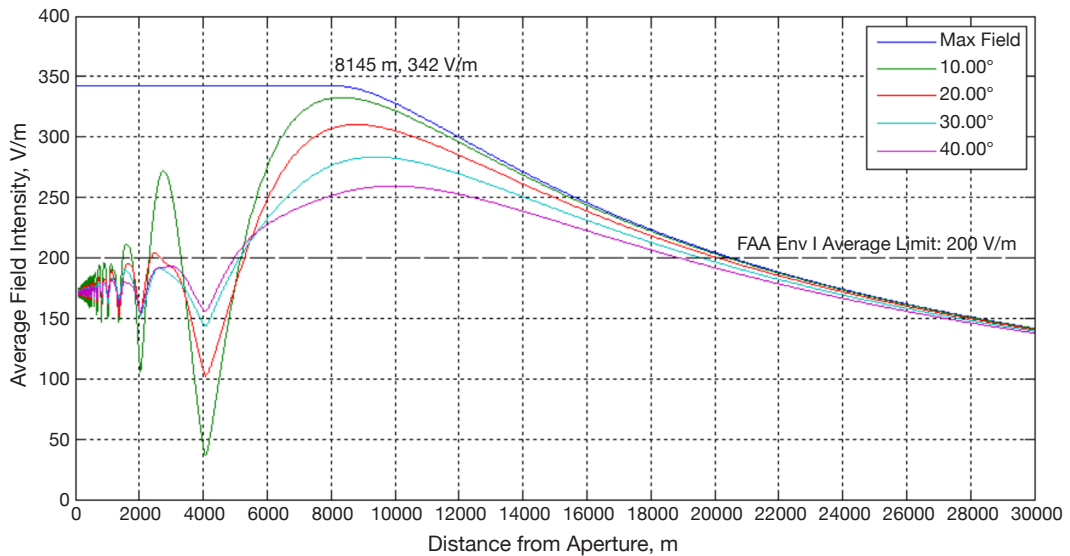


**Figure 4(d). Maximum and average field for 70-m, S-band, 400 kW, referenced to Environment I. Averaged field intensity over 1 s experienced by an aircraft at 100 knots, crossing the beam of a 70-m-aperture antenna at given angles (284000 W input power at 2.1 GHz).**

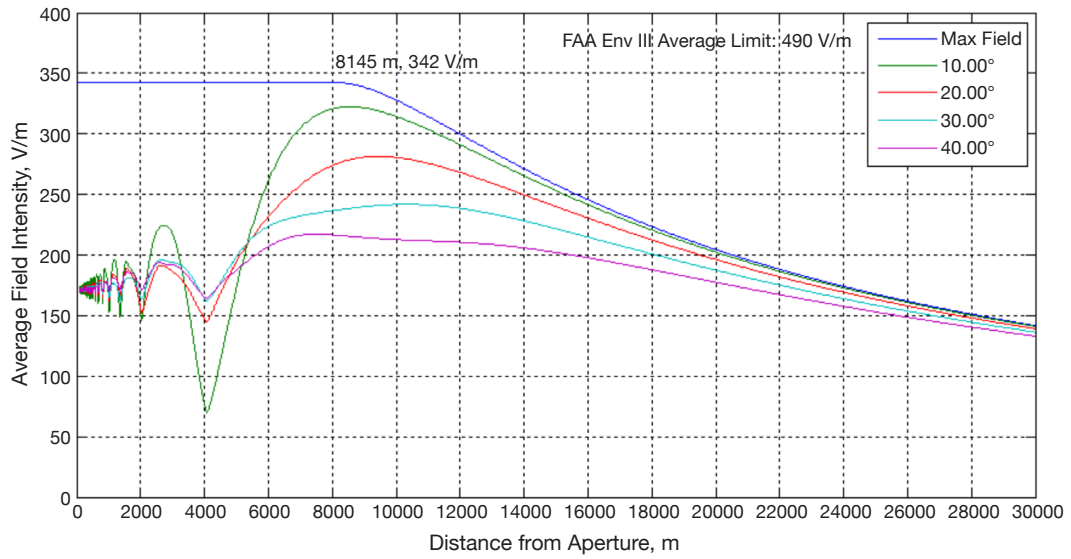


**Figure 4(e). Peak and average field for 70-m, S-band, 400 kW, referenced to Environment III. Averaged field intensity over 3 s experienced by a rotorcraft at 50 knots, crossing the beam of a 70-m-aperture antenna at given angles (284000 W input power at 2.1 GHz).**

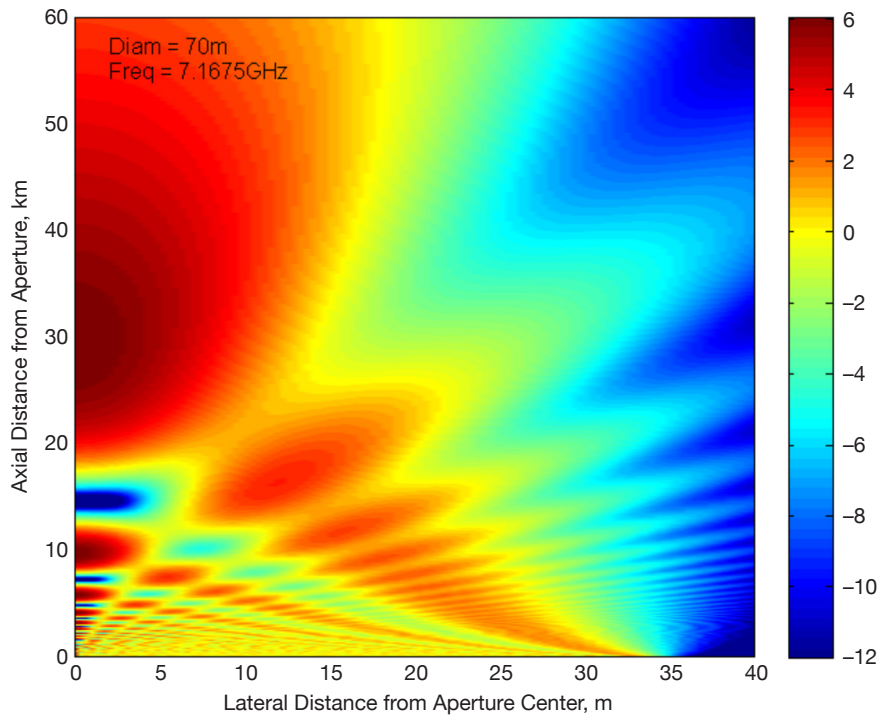


**Figure 5(a). Field structure for 70-m, 7.1 GHz (X-band), 20 kW: a color plot of normalized field power density in dB.**

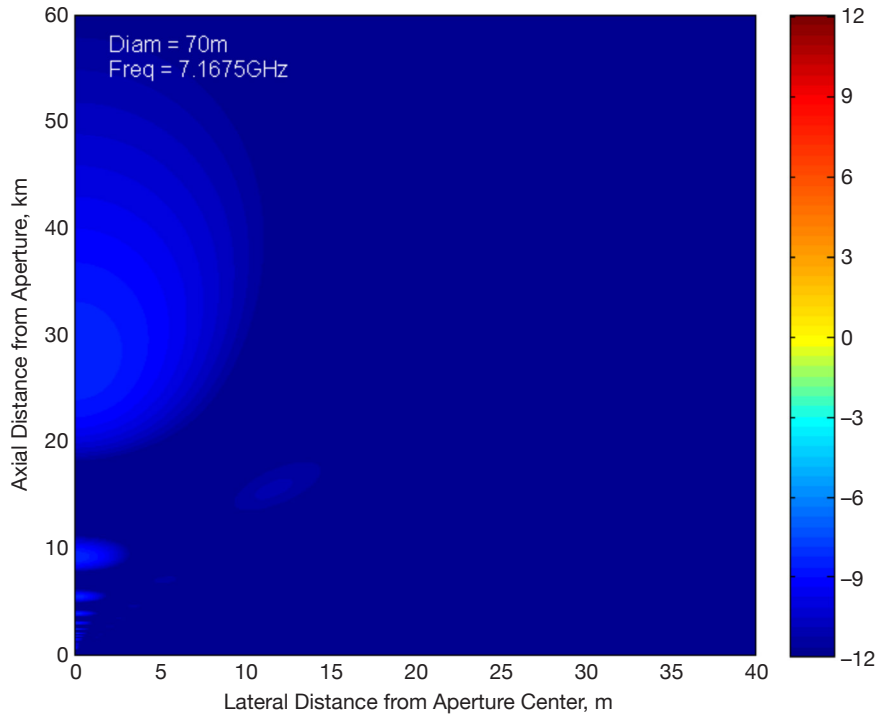


**Figure 5(b).** Field structure for 70-m, 7.1 GHz (X-band), 20 kW, referenced to Environment I. Field normalized to 200 V/m in dB for a 70-m circular-aperture antenna with 14200 W power at 7.1675 GHz.

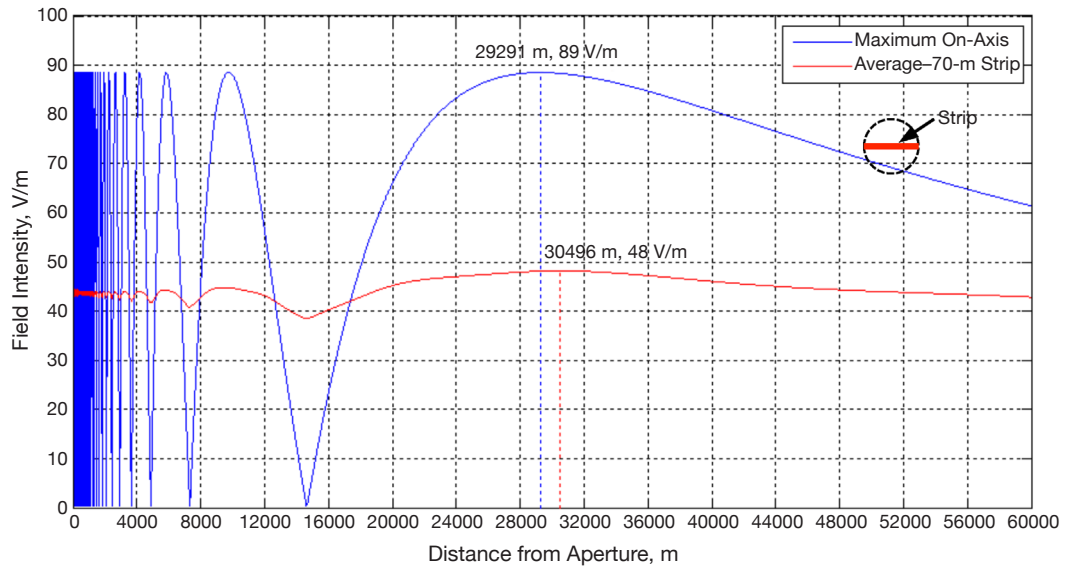


**Figure 5(c).** Maximum and average field for 70-m, 7.1 GHz (X-band), 20 kW. Averaged field intensity on a cross-section strip of given width for a 70-m-aperture antenna with 20000 W input power at 7.1675 GHz.

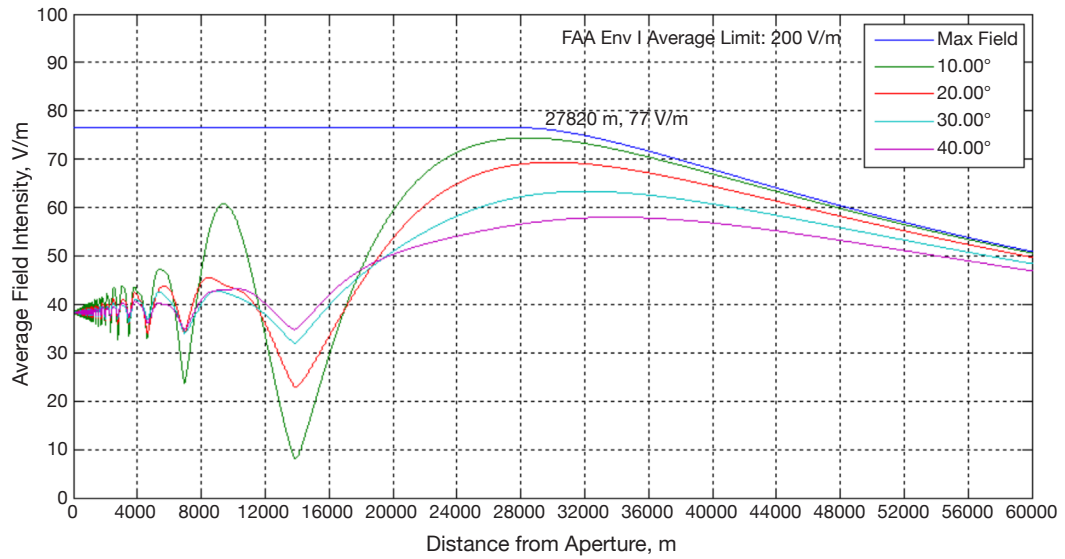


**Figure 5(d). Maximum and average field for 70-m, 7.1 GHz (X-band), 20 kW, referenced to Environment I. Averaged field intensity over 1 s experienced by an aircraft at 100 knots, crossing the beam of a 70-m-aperture antenna at given angles (14200 W input power at 7.1675 GHz).**

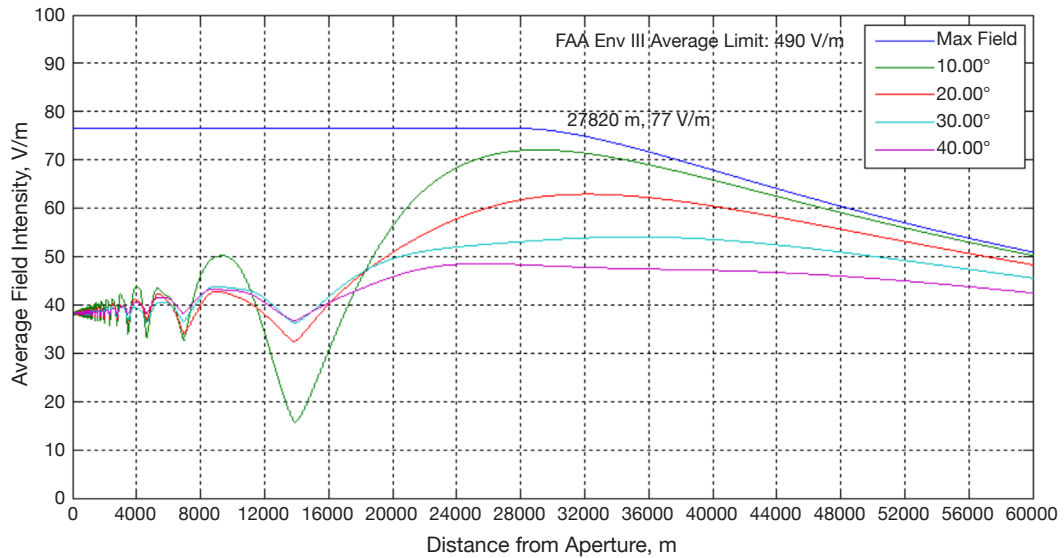


**Figure 5(e). Peak and average field for 70-m, 7.1 GHz (X-band), 20 kW, referenced to Environment III. Averaged field intensity over 3 s experienced by a rotorcraft at 50 knots, crossing the beam of a 70-m-aperture antenna at given angles (14200 W input power at 7.1675 GHz).**

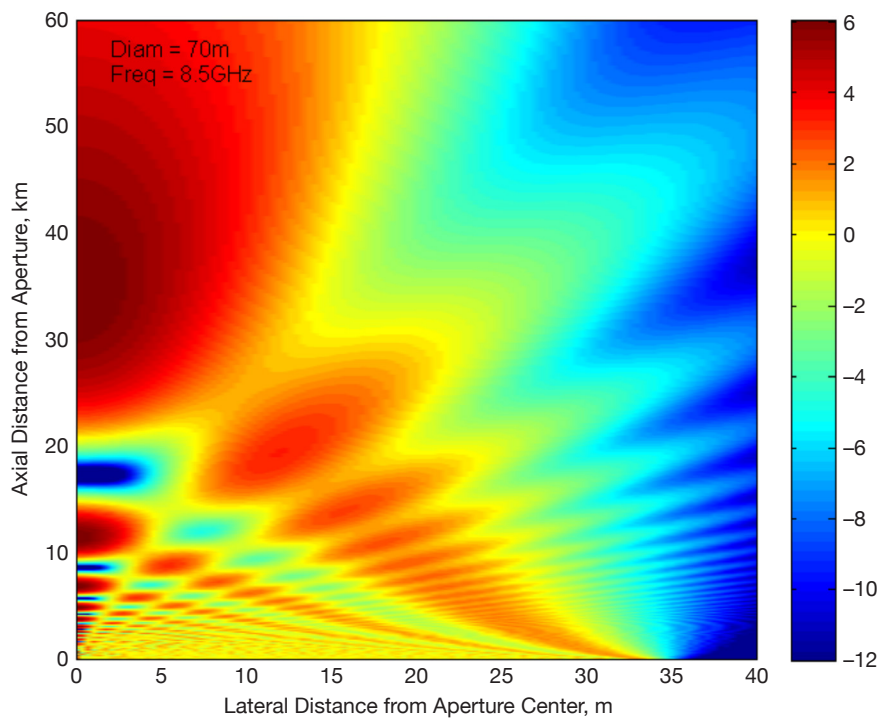


**Figure 6(a). Field structure for 70-m, 8.5 GHz (X-band), 500 kW: a color plot of normalized field power density in dB for a 70-m circular-aperture antenna at 8.5 GHz.**

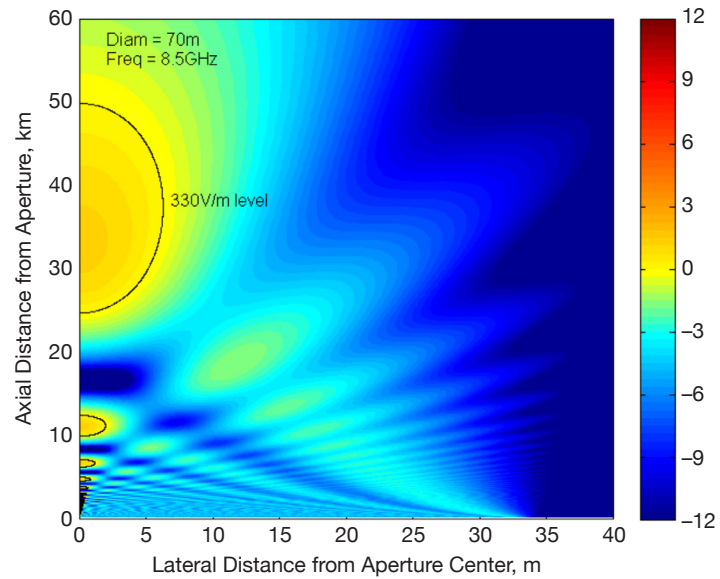
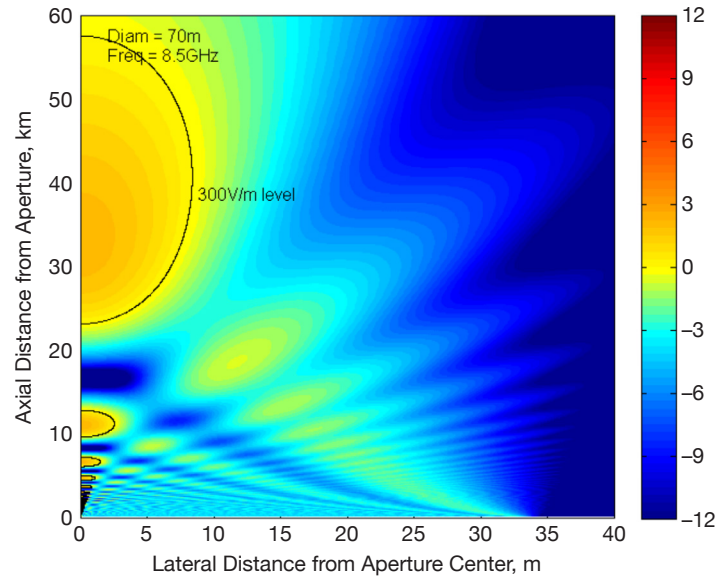


**Figure 6(b). Field structure for 70-m, 8.5 GHz (X-band), 500 kW: top, referenced to Environment I, field normalized to 300 V/m in dB for a 70-m circular-aperture antenna with 355000 W power at 8.5 GHz; bottom, referenced to Environment III, field normalized to 330 V/m in dB for a 70-m circular-aperture antenna with 355000 W power at 8.5 GHz.**

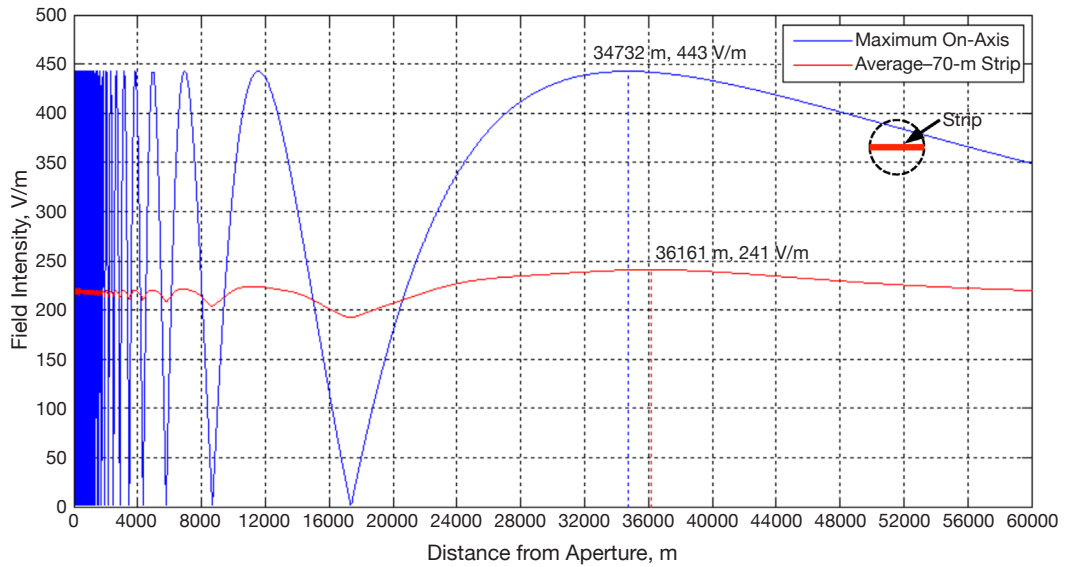


**Figure 6(c). Maximum and average field for 70-m, 8.5 GHz (X-band), 500 kW. Averaged field intensity on a cross-section strip of given width for a 70-m-aperture antenna with 5000000 W input power at 8.5 GHz.**

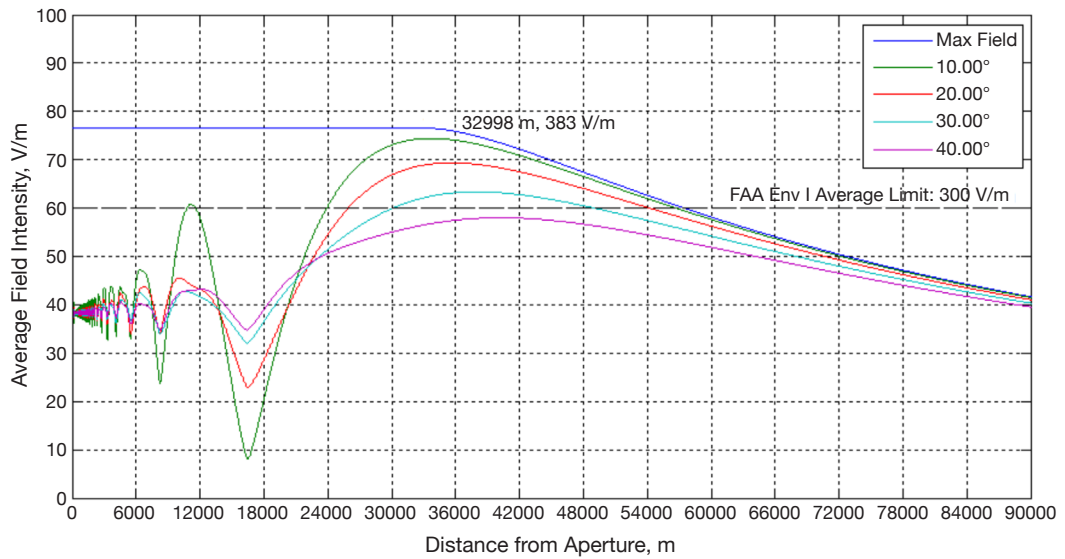


**Figure 6(d). Maximum and average field for 70-m, 8.5 GHz (X-band), 500 kW, referenced to Environment I. Averaged field intensity over 1 s experienced by an aircraft at 100 knots, crossing the beam of a 70-m-aperture antenna at given angles (355000 W input power at 8.5 GHz).**

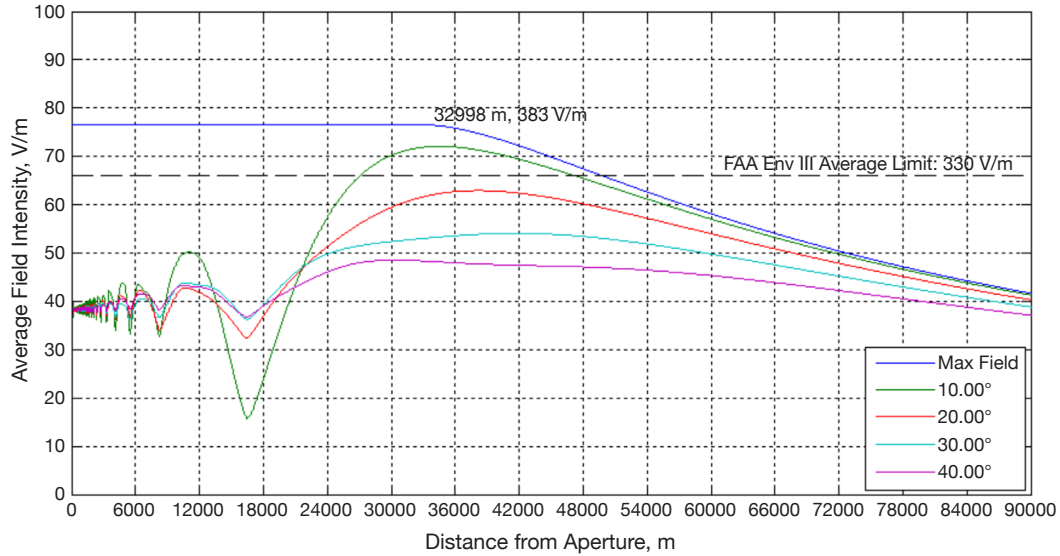


**Figure 6(e). Peak and average field for 70-m, 8.5 GHz (X-band), 500 kW, referenced to Environment III. Averaged field intensity over 3 s experienced by a rotorcraft at 50 knots, crossing the beam of a 70-m-aperture antenna at given angles (355000 W input power at 8.5 GHz).**

**Table 5(a). FAA requirements and calculated values, fixed-wing aircraft, Environment I.**

Emitter				DSN, V/m		FAA, Vm	
Diameter, m	Band	GHz	kW	Peak	Avg	Peak	Avg
34	X	7.1	80	316	283	1000	200
34	S	2.1	20	158	142	3000	200
70	S	2.1	400	342	333	3000	200
70	X	7.1	20	77	75	1000	200
70	X	8.5	500	383	372	3000	200

**Table 5(b). FAA requirements and calculated values, rotorcraft, Environment III.**

Emitter				DSN, V/m		FAA, Vm	
Diameter, m	Band	GHz	kW	Peak	Avg	Peak	Avg
34	X	7.1	80	316	255	1100	170
34	S	2.1	20	158	128	6000	490
70	S	2.1	400	342	323	6000	490
70	X	7.1	20	77	73	1100	170
70	X	8.5	500	383	361	5000	330

#### IV. Concluding Remarks

This article presents the results of the analyses of the DSN transmitters for HIRF applications. The methodology and the assumptions used in the DSN emitter analyses are consistent with the HIRF environment evaluation and assumptions used in the literature. The analysis presented here has been applied to other combinations of transmitters and antenna in the DSN, and has been incorporated into a published procedure.<sup>1</sup>

#### Acknowledgments

The author would like to acknowledge the immense contributions of Joseph Statman of the DSN project office in providing help in formulation of the problem, technical direction, as well as financial support for this work. The helpful discussions and encouragements of Wendy Hodgin of the project office are also appreciated.

#### References

- [1] R. W. Bickmore and R. C. Hansen, "Antenna Power Densities in the Fresnel Region," *Proceedings of IRE*, vol. 47, pp. 2119–2120, December 1959.
- [2] M. M. Rabello and S. L. G. Nobili, "Radiating Near-Field Power Density and Directivity Reduction of Tapered Circular Apertures," *Radio Science*, vol. 8, no. 7, pp. 677–680, July 1973.
- [3] *High-Intensity Radiated Field External Environments for Civil Aircraft Operating in the United States of America*, Naval Air Warfare Center, Aircraft Division, Patuxent River, Maryland, Report No. NAWCADPAX—98-156-TM, December 1998.
- [4] V. Jamnejad, "A Study of Near to Far Fields of JPL Deep Space Network (DSN) Antennas for RFI Analysis," IEEE Aerospace Conference, Big Sky, Montana, March 6–13, 2004.

---

<sup>1</sup> *DSN Procedure for Analysis of Emitter High-Intensity Radiated Fields*, DSN Document 842-50-357 (internal document), Jet Propulsion Laboratory, Pasadena, California, May 2012.

# Appendix

## Calculation of the Near to Mid Field of Large-Aperture Antennas

Obtaining the actual detailed fields of these antennas using rigorous physical optics, method of moments or other EM analysis techniques for large antennas at high frequencies is very complicated and time consuming. We have undertaken such a study, which will be the subject of another article, that also will compare those results with a simplified analysis given below.

There are a number of reports and papers on the subject of calculating the on-axis near field of large circular aperture antennas utilizing certain simplifications and approximations — see, e.g., [1,2]; additional information appeared in a JPL Interoffice Memorandum.<sup>2</sup> These provide maximum field values along the main/boresight axis of the antenna. Reference [3] in particular makes certain generalization for a variety of antennas, including the circular aperture antennas, which again provide a good summary of the on-axis field (detailed in Section 4.4 and more specifically in subsection 4.4.2.3 of that report). However, as can be shown, the field strength away from main axis becomes weaker. We have made a fairly rigorous but still approximate formulation in [4] to provide a more accurate representation of the field on and about the main beam of the antenna. And similar to previous papers, the following simplifying assumptions are made in obtaining the fields.

- (1) The pattern is circularly symmetric.
- (2) A scalar formulation for the field is used. The actual field is of a vectorial nature.
- (3) The field on the aperture is assumed to be uniform in amplitude. This is approximately valid, since the DSN dual-reflector antenna systems are shaped to produce a uniform phase and a fairly uniform amplitude distribution on the aperture with drop-off at the edges to reduce diffraction. We have used an effective uniformly illuminated aperture that is slightly smaller than the actual antenna (specifically, 33.09 for the 34-m antenna and 68.22 for the 70-m antenna).
- (4) The reflector is designed to produce uniform phase on the aperture. However, the surface errors, misalignments, gravity, and wind pressure effects will distort this uniform phase front. For the purpose of this study, we ignore these effects, although they can be included at a later stage.
- (5) The Fresnel approximation is made to the exponential kernel in the radiation integral such that the distance from observation point to a point on the aperture,  $r$ , is approximated by a linear term of the vertical distance to the aperture and a quadratic term of vertical distance to the central axis.

---

<sup>2</sup> D. A. Bathker, "Transmit Power Density for DSN 70-m and 34-m Dual-Shaped Antennas," JPL Interoffice Memorandum 3331-88-038 (internal document), Jet Propulsion Laboratory, Pasadena, California, April 5, 1988.

- (6) No blockage effects due to subreflector, support struts, etc., are directly included (but only through a lump-sum efficiency factor). They should have minimal effects.
- (7) No surface errors and tolerance are directly included in the computation process (but only through a lump-sum efficiency factor). These, in general, tend to reduce the peaks and partially fill the nulls in the field distribution.

The following parameters are defined and used in the calculations:

- Diameter of the aperture  $D = 2R$ , with  $R$  the radius
- Axial distance from the aperture,  $d$
- Radio frequency (RF),  $f$
- The wavelength,  $\lambda = c/f$  (for the frequency,  $f$ , and  $c = 299,792,458$  m/s)
- Characteristic distance from the aperture,  $d_c = 0.25D^2/\lambda = R^2/\lambda$   
(This distance is defined as the distance from the position of the last peak of the oscillating field along the main axis of the antenna to the antenna aperture, from which the point-field goes down smoothly towards the far field, as will be shown in the figures below.)
- Far-field limit distance from the aperture  $= 8 d_c = 2D^2/\lambda = 8R^2/\lambda$   
(A rather arbitrary definition of a distance from the aperture from which the path difference to the center and edge of the aperture are less than  $\lambda/16$ .)
- Normalized distance from the aperture,  $d_n = d/d_c$
- Total transmitted power,  $P_t$  (W)
- Power density at a given point,  $p$  (W/m<sup>2</sup>)
- Average power density on the aperture,  $p_a = P_t/(\pi R^2)$  (W/m<sup>2</sup>)
- Normalized power density at a given point,  $p_n = p/p_a$
- Gain at a given point,  $g$
- Peak gain of the antenna,  $g_0$
- Normalized gain at any point,  $g_n = g/g_0$

Several MATLAB programs are developed for the performance of calculations and obtaining subsequent plots.

The following observations are made based on the calculated data and resultant figures in the following pages. Figures A-1 to A-5 use normalized parameters applicable to any aperture diameter and frequency value. Figures A-5(a–c) are merely for graphical illustration and appreciation. As shown in Figure A-1, the envelope of power density along the central axis remains constant and 6 dB above the average power density on the aperture plane up to the distance  $d = d_c$  or  $d_n = d/d_c = 1$ . Thus, the normalized power density  $p_n = 6$  dB for  $d_n = d/d_c \leq 1$ . Subsequently, the power density goes down approximately as  $p_n = (\pi/d_n)^2$ .

Conversely, as shown in Figure A-2, the envelope of the gain along the central axis goes up from the aperture up to the distance  $d = d_c$  or  $d_n = 1$ , as  $g_n = (2d_n/\pi)_2$ . It then smoothly converges to peak gain  $g_0$ , or  $g_n = 1$ .

However, it should be noted that the actual field along the main axis has many nulls and peaks. In fact, only at limited points does the 6 dB value hold, but for a very large percentage of the length along the main axis, the field is less than or equal to the 0 dB or the average power density at the aperture.

In Figures A-3 and A-4, it can be seen that in a cross-section plane of the near-field beam with fixed distances from the aperture, and along lines parallel to the main axis, respectively, the power density oscillates more or less around the 0 dB value or the average power density at the aperture.

It is our considered opinion, based on other observations and experience, that in a real situation, including the aperture distribution taper, and more significantly, the surface errors, the field variations are dampened with lower peaks and partially filled nulls. In any case, the average field value across the beam with a base diameter of the size of the aperture is substantially lower than that on the main axis and much close to the average value on the aperture.

The results provided in the main body of this article are obtained from the formulation and developments outlined in this Appendix. It should be mentioned that they essentially agree with those of the previously cited JPL Interoffice Memorandum<sup>3</sup> along the main axis. That memorandum used certain assumptions in providing the efficiency and distribution of the power in the aperture. We have made some improvements on formulating and quantifying these assumptions that seem to be more accurate and more conservative for DSN antennas under consideration. Since the aperture distribution for the shaped reflector systems of the DSN 34- and 70-m antennas is nearly uniform and falls to very low levels towards the edges, we have assumed an effective uniform illumination diameter of 33.09 m for the 34-m antenna and 68.22 m for the 70-m antennas. The loss/efficiency factor at the aperture for all antennas is assumed to be 0.71 (1.5 dB), which is an upper bound for all cases.

---

<sup>3</sup> D. A. Bathker, "Transmit Power Density for DSN 70-m and 34-m Dual-Shaped Antennas," JPL Interoffice Memorandum 3331-88-038 (internal document), Jet Propulsion Laboratory, Pasadena, California, April 5, 1988.

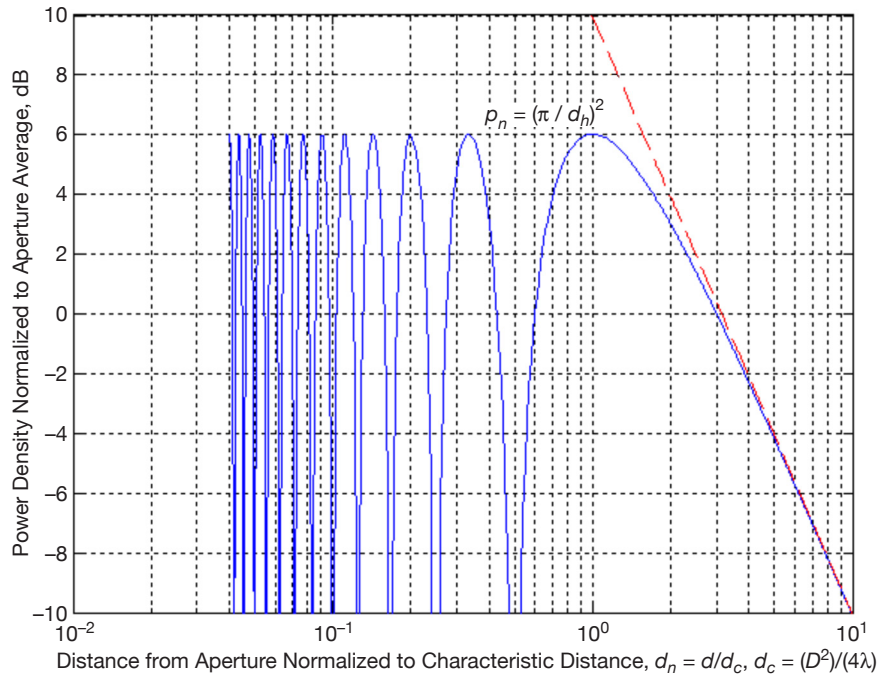


**Figure A-1. Normalized power density (to aperture average) along the boresight (main axis) of the antenna.**

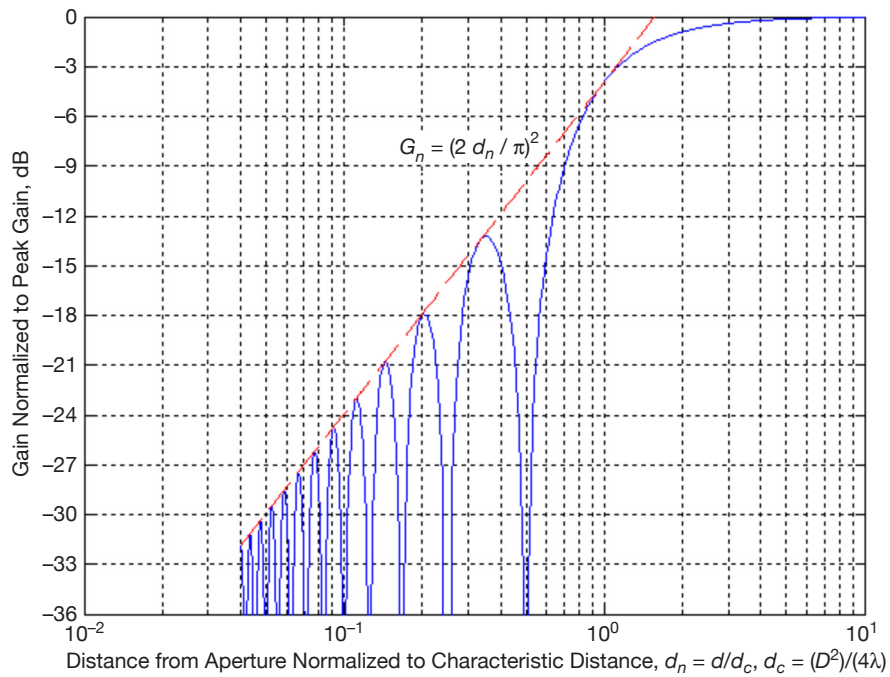


**Figure A-2. Normalized gain (to peak) along the boresight (main axis) of the antenna.**

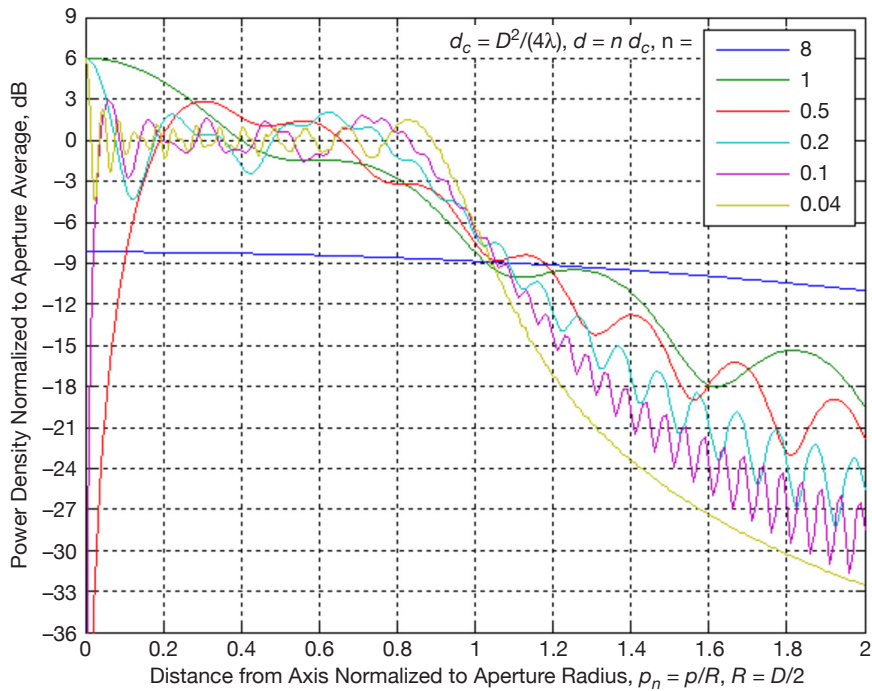


Figure A-3. Normalized power density (to aperture average) on planes of fixed distances from the aperture.

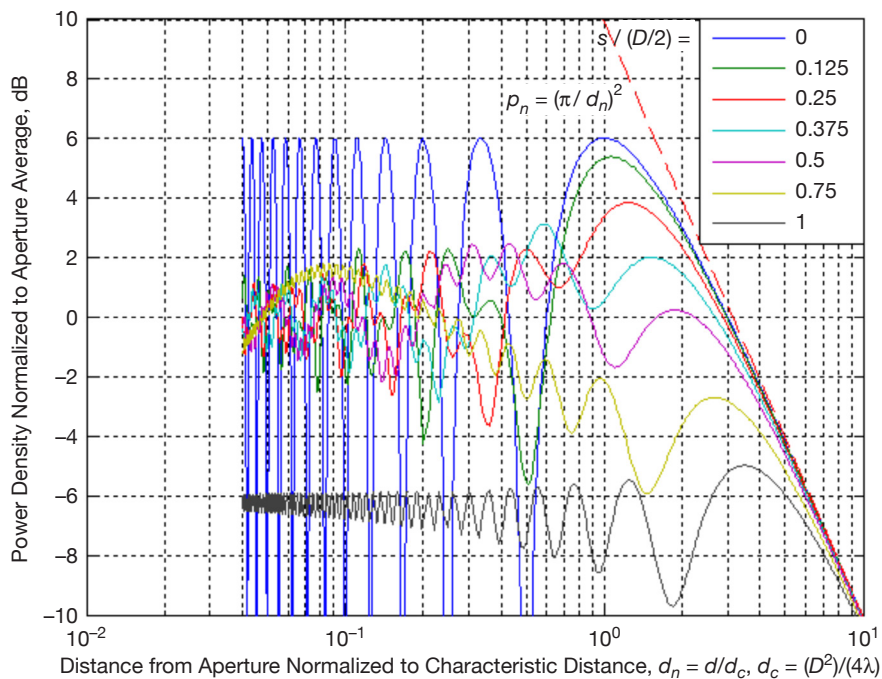
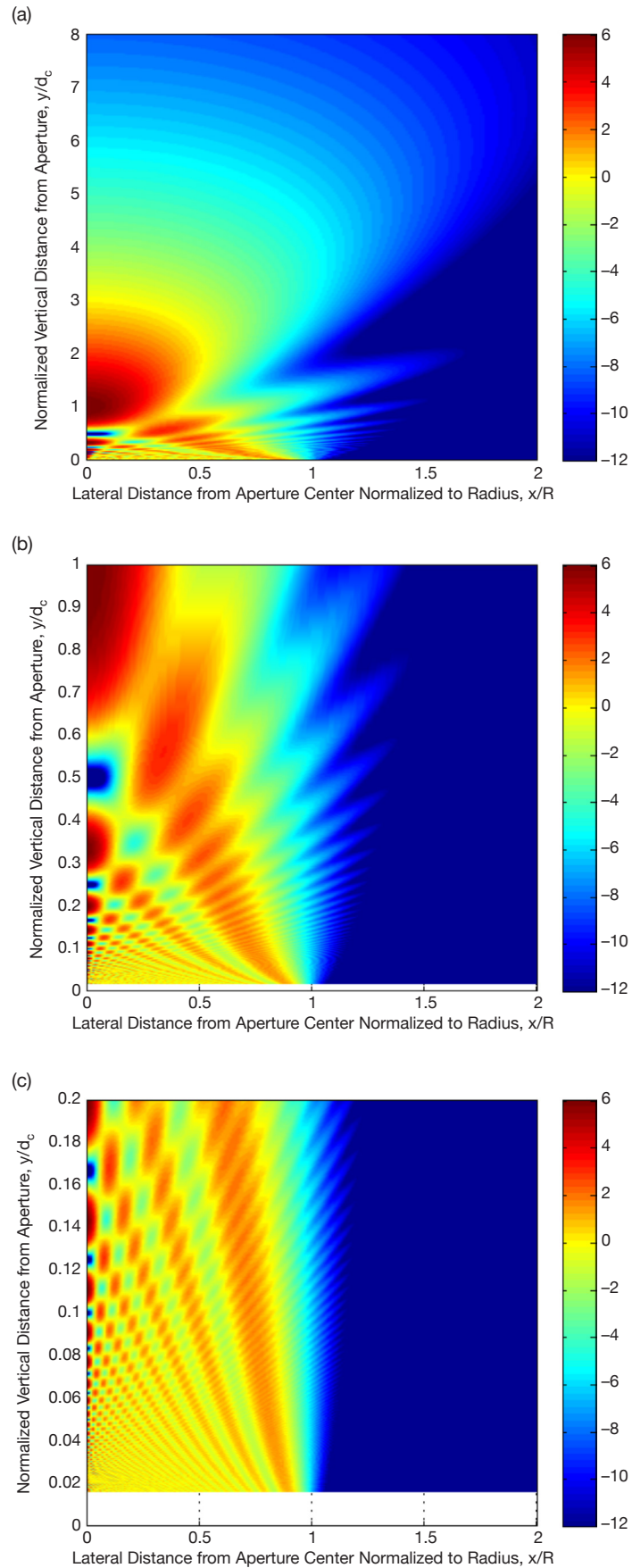


Figure A-4. Normalized power density (to aperture average) along lines parallel to the boresight axis.



**Figure A-5. Contour plot of normalized power density (dB) of aperture antenna: (a) for a distance of 0 to 8 times, (b) 0 to 2 times, and (c) 0 to 0.2 times the characteristic distance  $d_c = D^2/(4\lambda)$  along the antenna axis.**